Check for updates

Interplanetary mesoscale observatory (InterMeso): A mission to untangle dynamic mesoscale structures throughout the heliosphere

Robert C. Allen[1]*, Evan J. Smith[1], Brian J. Anderson[1],
Joseph E. Borovsky[2], George C. Ho[1], Lan Jian[3],
Sämuel Krucker[4], Susan Lepri[5], Gang Li[6], Stefano Livi[5],
Noé Lugaz[7], David M. Malaspina[8,9], Bennett A. Maruca[10,11],
Parisa Mostafavi[1], Jim M. Raines[5], Daniel Verscharen[12],
Juliana Vievering[1], Sarah K. Vines[1], Phyllis Whittlesey[13],
Lynn B. Wilson III[3] and Robert F. Wimmer-Schweingruber[14]

[1]Johns Hopkins University Applied Physics Lab, Laurel, MD, United States, [2]Center for Space Plasma
Physics, Space Science Institute, Boulder, CO, United States, [3]NASA Goddard Space Flight Center,
Heliophysics Science Division, Greenbelt, MD, United States, [4]Fachhochschule Nordwestschweiz,
Windisch, Switzerland, [5]Department of Climate and Space Sciences and Engineering, University of
Michigan, Ann Arbor, MI, United States, [6]Department of Space Sciences, University of Alabama in
Huntsville, Huntsville, AL, United States, [7]Space Science Center, University of New Hampshire,
Durham, NH, United States, [8]Astrophysical and Planetary Science Department, University of Colorado,
Boulder, CO, United States, [9]Labratory for Atmospheric and Space Physics, University of Colorado,
Boulder, CO, United States, [10]Department of Physics and Astronomy, University of Delaware, Newark,
DE, United States, [11]Bartol Research Institute, University of Delaware, Newark, DE, United States,
[12]Mullard Space Science Laboratory, University College London, Dorking, United Kingdom, [13]Space
Sciences Laboratory, University of California, Berkeley, Berkeley, CA, United States, [14]Insitute of
Experimental and Applied Physics, University of Kiel, Kiel, Germany

Mesoscale dynamics are a fundamental process in space physics, but fall within
an observational gap of current and planned missions. Particularly in the solar
wind, measurements at the mesoscales (100s R_E to a few degrees heliographic
longitude at 1 au) are crucial for understanding the connection between the
corona and an observer anywhere within the heliosphere. Mesoscale dynamics
may also be key to revealing the currently unresolved physics regulating particle
acceleration and transport, magnetic field topology, and the causes of variability
in the composition and acceleration of solar wind plasma. Studies using single-
point observations do not allow for investigations into mesoscale solar wind
dynamics and plasma variability, nor do they allow for the exploration of the
sub-structuring of large-scale solar wind structures like coronal mass ejections
(CMEs), co-rotating/stream interaction regions (CIR/SIRs), and the heliospheric
plasma sheet. To address this fundamental gap in our knowledge of the
heliosphere at these scales, the Interplanetary Mesoscale Observatory
(InterMeso) concept employs a multi-point approach using four identical
spacecraft in Earth-trailing orbits near 1 au. Varying drift speeds of the
InterMeso spacecraft enable the mission to span a range of mesoscale
separations in the solar wind, achieving significant and innovative science

return. Simultaneous, longitudinally-separated measurements of structures co-rotating over the spacecraft also allow for disambiguation of spatiotemporal variability, tracking of the evolution of solar wind structures, and determination of how the transport of energetic particles is impacted by these variabilities.

Introduction

The solar wind is a multi-scale and highly dynamic system with interplay between the micro-, meso-, and macro-scales. Decades of single-point observations have led to great insight into the large-scale variability in the solar wind and its transient phenomena, such as coronal mass ejections (CMEs), stream and co-rotating interaction regions (SIR/CIRs), and solar energetic particle (SEP) events associated with flares and/or CMEs. These observations have revealed differences between high-speed streams originating from coronal holes, typical slow solar wind, and Alfvénic slow solar wind (see D'Amicis et al., 2019) and established the current paradigm under which the solar wind is interpreted today.

Previous studies from the Solar Terrestrial Relations Observatory (STEREO) mission and other serendipitous multi-point observations have allowed investigations of spatial variations of the solar wind and transients over large distances. For instance, the radial evolution of the expanding solar wind has been studied statistically using observations from Helios (Perrone et al., 2019), while the radial evolution of CIRs has been studied within the orbit of Earth (e.g., Richter and Luttrell, 1986; Schwenn, 1990; Jian et al., 2008; Allen et al., 2021a; Allen et al., 2021b) and between Earth and Mars (e.g., Geyer et al., 2021). Multi-point observations of CIRs, and their associated energetic particles, over large longitudinal separations have also revealed significant temporal evolution of the structures as they corotate over 10s of degrees longitude (Mason et al., 2009; Jian et al., 2019; Allen et al., 2021a). Additionally, radial (e.g., Burlaga et al., 1981; Liewer et al., 2020) and longitudinal (e.g., Kilpua et al., 2009; Farrugia et al., 2011; Kollhoff et al., 2021) studies of CME structures have found significant variations over these large separations.

On smaller, ion kinetic scales (<1,000 km), the solar wind and transients have been found to be highly turbulent and structured, with clear signs of coupling processes over a large range of spatiotemporal scales (e.g., Bandyopadhyay et al., 2018; Roberts et al., 2020). While the Magnetospheric Multiscale (MMS) and Cluster missions, designed to target kinetic scales, have demonstrated the importance and richness of small-scale and highly dynamic plasma processes, these scales are "on the receiving end" of the turbulent cascade that is driven by the large-scale solar wind structures (Verscharen et al., 2019). As such, the intermediate scale, between the small, kinetic scale dynamics explored by MMS and Cluster, and the larger scale structuring and variations observed by STEREO and multi-

mission comparisons, represents the critical scale needed to understand cross-scale processes in the solar wind. This intermediate scale—the mesoscale—is crucial for understanding the connection of the corona to an observer anywhere within the heliosphere, as well as for revealing the currently unresolved physics regulating particle transport, magnetic field topology, and the variability in composition and acceleration of solar wind plasma.

The mesoscale solar wind currently falls within a gap both observationally and in spatiotemporal scales of current simulations, and as such is a critical missing link in our fundamental understanding of the heliosphere. A new mission targeting this critical gap of mesoscale dynamics would enable investigations into how solar sources imprint themselves into the solar wind at 1 au and beyond *via* mesoscale structuring, how mesoscale variability evolves as it propagates from the Sun, and how the intrinsic structure of the solar wind impacts the structure of transients and particle acceleration and transport. The mesoscale regime of the solar wind may likely be the missing piece to long sought questions of sources of solar wind, particle acceleration, and particle transport. Gaining the ability to probe the mesoscale solar wind will allow for leaps in our understanding of these outstanding questions.

InterMeso science objectives and motivation

To address the overarching science objective of Investigating the fundamental mesoscale nature of the variable solar wind and its impacts on particle acceleration, evolution, and transport, the Heliophysics community requires a mission to: 1) Characterize and identify the origin of the mesoscale variability of the background solar wind and transient solar wind structures and 2) Characterize and understand the impact of these mesoscale variations on particle acceleration and transport.

Objective 1: Characterize and identify the origin of the mesoscale variability of the background solar wind and transient solar wind structures

The solar surface exhibits structure on granule and supergranule scales (shown by the model results in
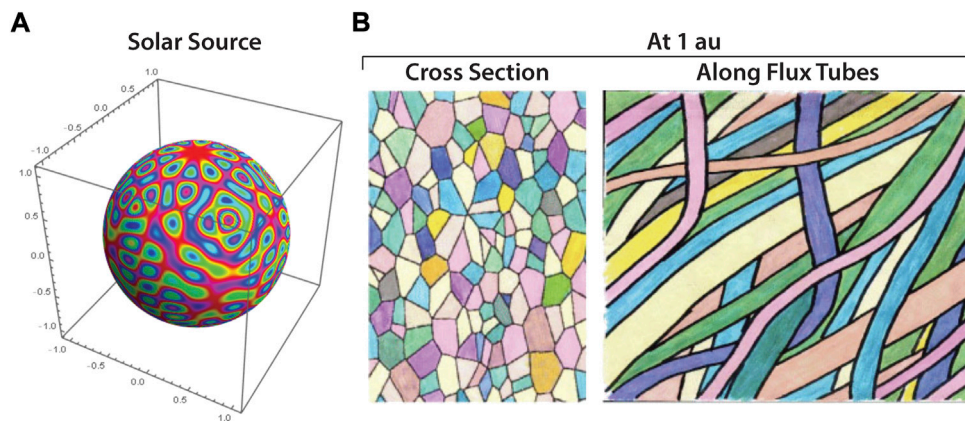
FIGURE 1
(A) Modeled representation of typical topology of magnetic structures on the solar surface (adapted from Bian and Li, 2021). **(B)** As these structures convect outward to 1 au, they can undergo processes such as expansion and stochastic meandering, but may preserve their characteristics as granule to supergranule relics on the Sun (cartoon adapted from Borovsky, 2008). The nature of flux tube structure at 1 au remains a fundamental open question.
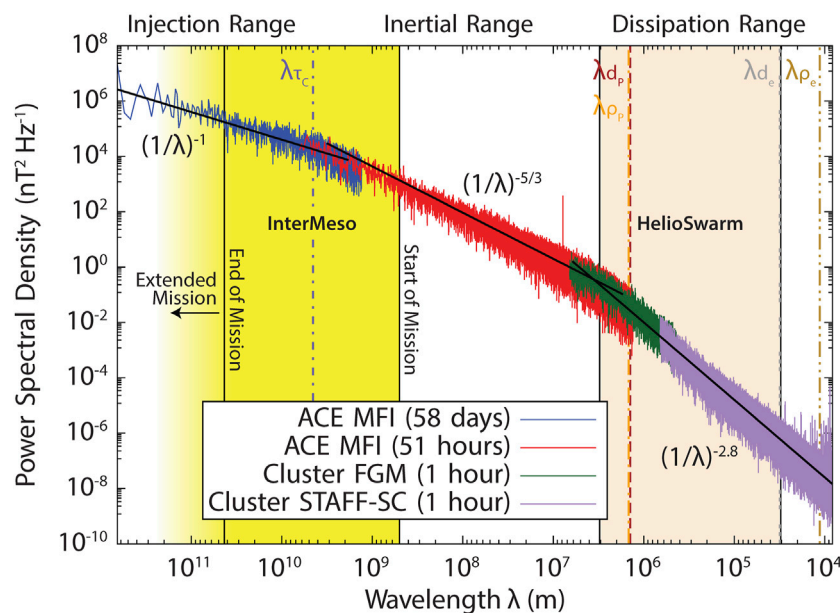
FIGURE 2
The power spectral density of magnetic field fluctuations at time of solar wind plasma beta near 1 au shows two spectral breaks (see Verscharen et al., 2019). The injection range is characterized by a power spectral density slope of $(1/\lambda)^{-1}$, while the inertial range has a slope of $(1/\lambda)^{-5/3}$ in the spacecraft frame. The critical frequencies marked are the correlation length ($f_{\tau c}$), proton inertial length (f_{dp}) and ion-gyro scale ($f_{\rho p}$), and the electron inertial length (f_{de}) and electron-gyro scale ($f_{\rho e}$). While the upcoming HelioSwarm mission will explore the transition between the inertial and dissipation ranges (tan region), InterMeso, for the first time, will reveal the spatiotemporal dynamics between the injection and inertial range (yellow region). Adapted from Verscharen et al. (2019).

Figure 1A). As solar magnetic structures convect out with the solar wind, they can undergo meandering due to footpoint motion, reconnection, and, possibly more importantly at 1 au, stochastic motion and turbulent evolution (e.g., Borovsky, 2008; Ashraf and Li, 2019; Bian and Li, 2021). As such, once flux tubes reach 1 au, they can be tangled into a complex meso-structure (illustrated in Figure 1B) (Borovsky, 2008). These processes and structuring can lead to various effects, such as "dropout"

FIGURE 3
(A) Relevant scale sizes of CME structures at 1 au (from Ala-Lahti et al., 2020). The fraction of 20−126 keV ion time intensity profiles that remain unchanged between two observing points as a function of spacecraft separation both **(B)** in the plane of the shock and **(C)** along the shock normal shows distinct variability that may be related to the variable scale sizes of CME sub-structuring (from Neugebauer et al., 2006). The mesoscale structuring and subsequent effects on particle acceleration remain outstanding open questions in Heliophysics.
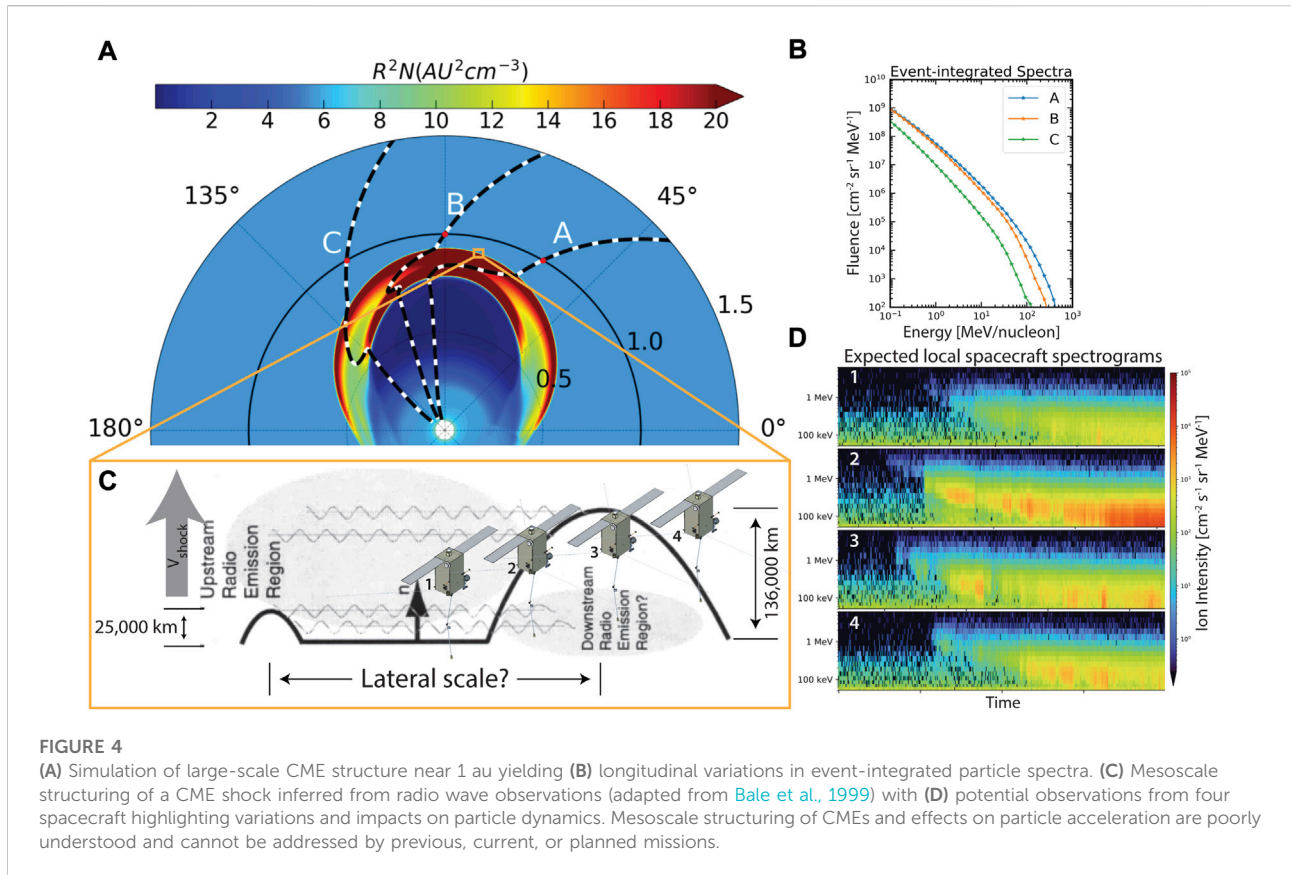
phenomena in energetic particles (Mazur et al., 2000). However, the fundamental structuring and coherence of flux tubes in interplanetary space remain largely unknown.

Moving from the large-scale structures to mesoscale and smaller ranges, the nature of injection range fluctuations in the solar wind is not well understood, nor is the transition at the break point between the injection range and the inertial range (see the review by Verscharen et al., 2019). Persistent, large-scale structures may transition to dynamic structures at scales near 10^9–10^{10} m (Figure 2). However, this critical transitory scale between injection range and inertial ranges has been elusive from a single-spacecraft vantage point, as these observations are limited in the ability to distinguish temporal variations and those resulting from convection of spatially-variable solar wind over an observer. While the currently planned HelioSwarm mission will, for the first time, robustly explore the spatiotemporal transition between the inertial range and dissipation range, the injection-to-inertial range transition will remain unexplored. HelioSwarm is a NASA Heliophysics Medium-Class Explorer (MIDEX) mission currently in development that aims to study solar wind turbulence (at scales of 50–3,000 km), and consists of nine spacecraft (one hub and eight node spacecraft) in a lunar resonant orbit (see https://eos.unh.edu/helioswarm/mission for additional details).

Only through multi-point observations with separations on the order of this critical scale can we robustly explore this fundamental transition in the solar wind.

In addition to the currently unconstrained, fundamental mesoscale structuring of the solar wind, sub-structuring of transient events is also not well understood. The small number of studies that have utilized fortuitous, but sporadic, multi-mission conjunctions to investigate the mesoscale structuring of CME shocks have shown that CME-associated shocks and magnetic ejecta have smaller-scale structuring, although the degree of such structuring is largely not understood (e.g., Bale et al., 1999; Knock et al., 2003; Pulupa and Bale, 2008; Koval and Szabo, 2010; Lugaz et al., 2018). As shown in Figure 3A, the various scale lengths of the solar wind, CME sheath, and CME ejecta are expected to be different from one another (Ala-Lahti et al., 2020). Additionally, comparisons of shocks between the Advanced Composition Explorer (ACE) and Wind missions have found that energetic particle time-intensity profiles often change over mesoscales indicating important effects of mesoscale structuring on particle acceleration and transport (Figures 3B,C, Neugebauer et al., 2006). Observations such as these indicate that the "large-scale-only" view of the solar wind is an incomplete picture of the fundamental structure of the solar wind and the important

FIGURE 4
(A) Simulation of large-scale CME structure near 1 au yielding **(B)** longitudinal variations in event-integrated particle spectra. **(C)** Mesoscale structuring of a CME shock inferred from radio wave observations (adapted from Bale et al., 1999) with **(D)** potential observations from four spacecraft highlighting variations and impacts on particle dynamics. Mesoscale structuring of CMEs and effects on particle acceleration are poorly understood and cannot be addressed by previous, current, or planned missions.

processes that define its evolution. Dedicated multi-point observations are needed to reveal these fundamental physical processes.
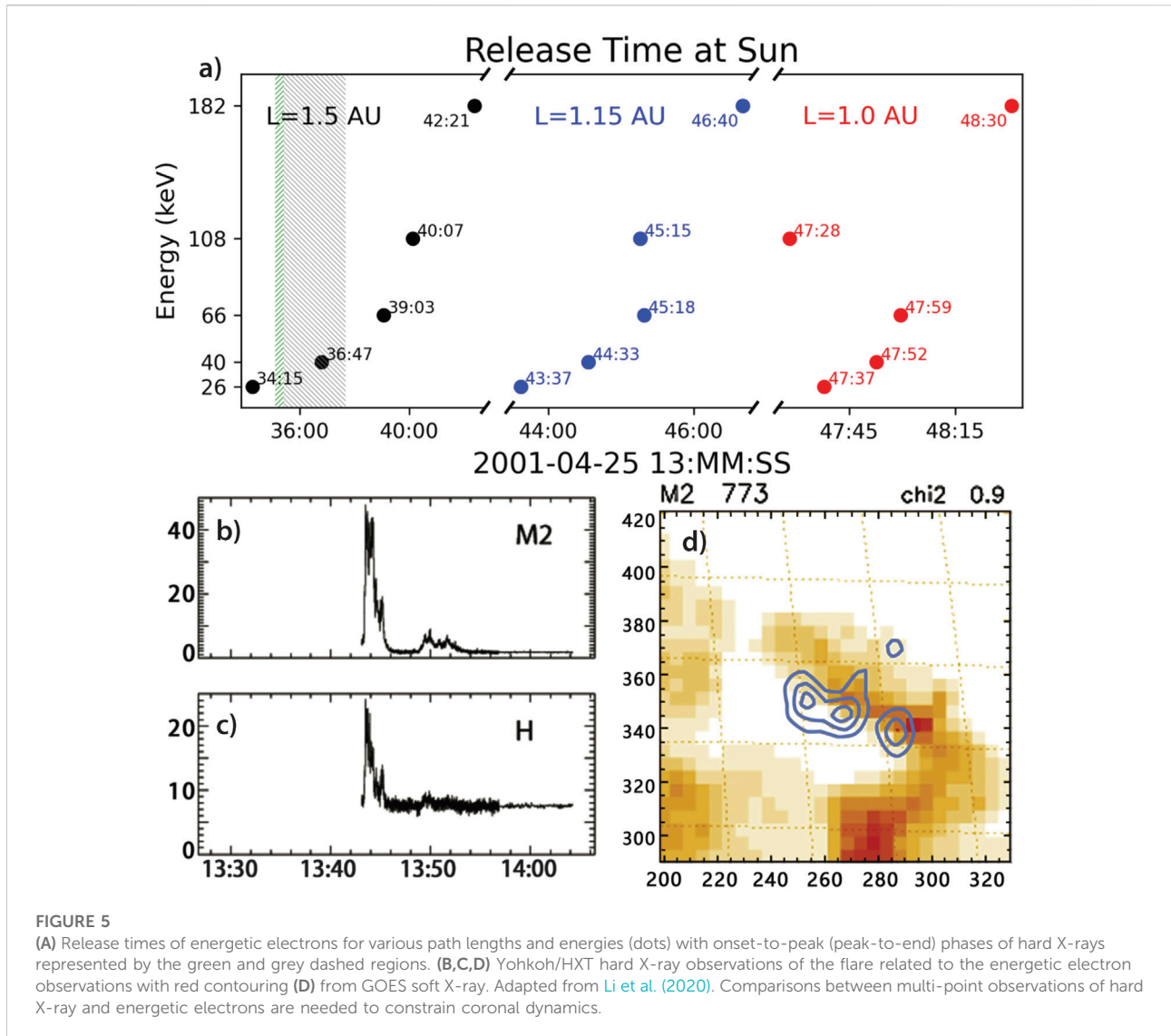
Objective 2: Characterize and understand the impact of these mesoscale variations on particle acceleration and transport

Particle acceleration is fundamentally dependent upon local conditions in the acceleration regions and, as such, mesoscale variations in the solar wind and along/within transients will affect acceleration processes. For example, a CME expanding into solar wind streams with spatial pressure variations may lead to deformation of its structure (e.g., Owens et al., 2017), resulting in spatially varying shock structure in the mesoscale range. Such mesoscale variations along a shock surface lead to localized differences in shock parameters affecting particle acceleration, and so could potentially explain the variations observed in Figures 3B,C. Detailed observations at multiple points along such structures are required to determine the mesoscale effect on CME particle acceleration.

Radio wave observations have demonstrated the presence of mesoscale variations in shock structure (e.g., Bale et al., 1999;

Figure 4C); however, it remains unknown to what degree the mesoscale structuring affects particle acceleration. While current models can reproduce large-scale variation in event-integrated particle spectra along an interplanetary shock (Figures 4A,B), which have been observed by conjunctions of spacecraft at large separations (e.g., Hu et al., 2018), these approaches are unable to capture the effects of mesoscale structuring or short time cadence evolution (Figure 4D). For example, an event-integrated spectra includes particles accelerated from various locations along the shock structure, but the seed populations and freshly accelerated ions will be more localized to the mesoscale variations of the structure. Better understanding the role that mesoscale structure plays in controlling the variability of particle acceleration along an interplanetary shock is critical for investigating the causes of observed variation between events and potential seed populations.

Additionally, our understanding of flare acceleration of energetic electrons will be greatly advanced through a robust exploration of mesoscale particle variations. For instance, Li et al. (2020) found that the injection timing of energetic electrons compared to hard X-ray observations suggests the presence of two distinct electron populations in an impulsive solar energetic electron event (Figure 5). The presence or absence of these electron populations can differentiate

FIGURE 5
(A) Release times of energetic electrons for various path lengths and energies (dots) with onset-to-peak (peak-to-end) phases of hard X-rays represented by the green and grey dashed regions. **(B,C,D)** Yohkoh/HXT hard X-ray observations of the flare related to the energetic electron observations with red contouring **(D)** from GOES soft X-ray. Adapted from Li et al. (2020). Comparisons between multi-point observations of hard X-ray and energetic electrons are needed to constrain coronal dynamics.

between different types of magnetic reconnection at the flare site (e.g., interchange reconnection versus reconnection between two closed field lines). However, the determination of the path length that the energetic electrons traversed from the flare to the observer is the primary source of ambiguity in these observations, which may be a result of mesoscale variations impacting particle transport. For example, field line meandering and/or stochastic motion can lead to uncertainties of where a source region maps to of up to $10°$ in longitude at 1 au (Figure 6B, Bian and Li, 2021). Observing energetic electrons at multiple spacecraft with a close separation (<$10°$ total span) will allow for the determination of acceleration time scales of electrons at solar flares, through fractional dispersion analysis (FVDA, Zhao et al., 2019) or other analysis techniques, and so for differentiating among proposed reconnection mechanisms.

The complexities of transport between the corona and 1 au are apparent in impulsive SEP events. For example, when the two STEREO spacecraft were within $34°$ heliographic longitude of one another in 2014 (Figure 7A), a flare event occurred at an active region near the footpoints of both spacecraft (Figure 7B). During this event, as shown in Figure 7C, STEREO-A, despite the footpoint being slightly further from the active region, observed a higher peak in 55–65 keV electron intensity with an onset time about an hour earlier, and with higher anisotropy, than STEREO-B (Klassen et al., 2016). Because transport of flare-accelerated energetic electrons depends on background solar wind structure, particle acceleration at flare sites, and the mechanisms driving cross-field diffusion, this event presents a clear example of the importance of mesoscale variations on the transport of energetic electrons from the flare site in the corona to 1 au. As such, a robust multi-point investigation at mesoscale separations is
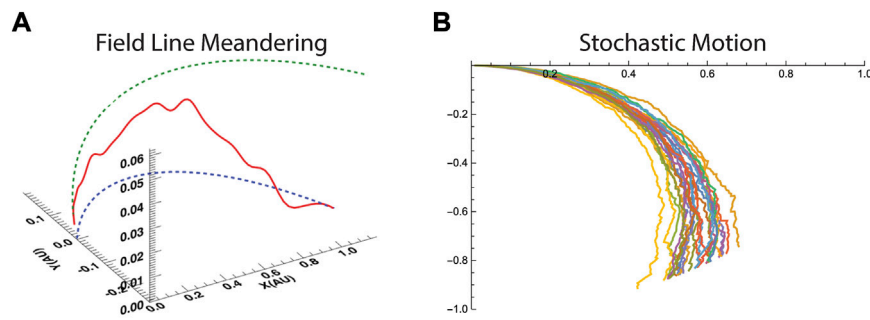
FIGURE 6
(A) Field line meandering (from Ashraf and Li, 2019) and **(B)** stochastic motion (from Bian and Li, 2021) are important mechanisms that cause the location of energetic electrons reaching 1 au to dramatically deviate from the nominal Parker Spiral. The relative contributions of these processes on particle transport are unknown, but critical to understanding particle dynamics.

required to disentangle the complexities of particle transport in the inner heliosphere.

For particle transport from local acceleration sites associated with transients, mesoscale variations may also play an important role. As energetic particles propagate along a field line away from an acceleration site, such as from reverse shocks at CIRs, various processes (e.g., adiabatic cooling and particle scattering) leading to hardening of the lower-energy spectra are thought to occur (e.g., Fisk and Lee, 1980). However, this spectral hardening has not been observed as often, or as significantly, as expected (e.g., Mason and Sanderson, 1999; Desai et al., 2020; Allen et al., 2021a; Joyce et al., 2021). To explain this discrepancy, several theories have been developed, such as compressive, non-shock related acceleration (e.g., Giacalone et al., 2002; Fisk and Gloeckler, 2006; Ebert et al., 2012; Chen et al., 2015) and/or modifications to the magnetic topology, such as sub-Parker spirals (e.g., Murphy et al., 2002; Schwadron, 2002; Schwadron et al., 2020).

While these other processes may explain the observed weak modulation of the particle spectra, a CIR observation utilizing a fortuitous multi-spacecraft vantage point seems to suggest strong path length-dependent modulation (Zhao et al., 2016; Figures 8A,B). In this event, a CIR shock was observed at STEREO-B when it was ~23° from Earth, however the shock was not observed at ACE, and the CIR evolved too significantly relative to STEREO-A for comparison. STEREO-B and ACE measurements indicate strong path-dependent modulation of the observed particle spectra (Figure 8B). However, the required assumption of negligible temporal evolution of the CIR between observations does not fully capture the possible variations of the shock and dynamics regulating particle acceleration and transport, adding ambiguity to the findings. Constraining the true path length to the reverse shock and spatiotemporal variations of shock-related acceleration is difficult with single point observations. Only simultaneous, multi-point observations from different points within a CIR and its rarefaction region allows for differentiation between path-

length dependent modulation and competing transport and acceleration processes.

Significance, impact, and timeliness

Fundamentally understanding the mesoscale (100s R_E to a few degrees heliographic longitude at 1 au, i.e., in-between the inertial and injection ranges) structure of the solar wind and transients and its subsequent effects on particle acceleration and transport will be paradigm shifting in our insight into the heliosphere, as mesoscale dynamics are vital for resolving long-standing questions of the community. As such, a new mission with an enabling, multi-point architecture is essential to address these objectives. InterMeso will fill a critical observational gap in the current Heliophysics System Observatory (HSO) as mesoscale solar wind structure and dynamics falls between the global scales studied by the *in situ* instrumentation on STEREO (Kaiser et al., 2008) and occasional opportune conjunctions within the HSO, and the kinetic-scales unlocked by MMS (Burch et al., 2016), Cluster (Escoubet et al., 2001), and the HelioSwarm mission (illustrated in Figure 9).

The goal of InterMeso, to resolve the critical physics and consequences of the mesoscale solar wind and transients, is also particularly timely for the next decade. With the continued operation of ground-based solar observatories (e.g., Daniel K. Inouye Solar Telescope, DKIST; Tritschler et al., 2016) and solar/heliographic imaging satellite missions, InterMeso measurements will have complementary remote sensing observations of the solar footpoints of the spacecraft. The upcoming discoveries from the Polarimeter to Unify the Corona and Heliosphere (PUNCH; https://punch.space.swri.edu/) mission will enable a better understanding of the initial mesoscale structuring of the coronal young solar wind, and so will feed directly into the interpretations of mesoscale variability at 1 au from InterMeso, furthering our insight into the evolution
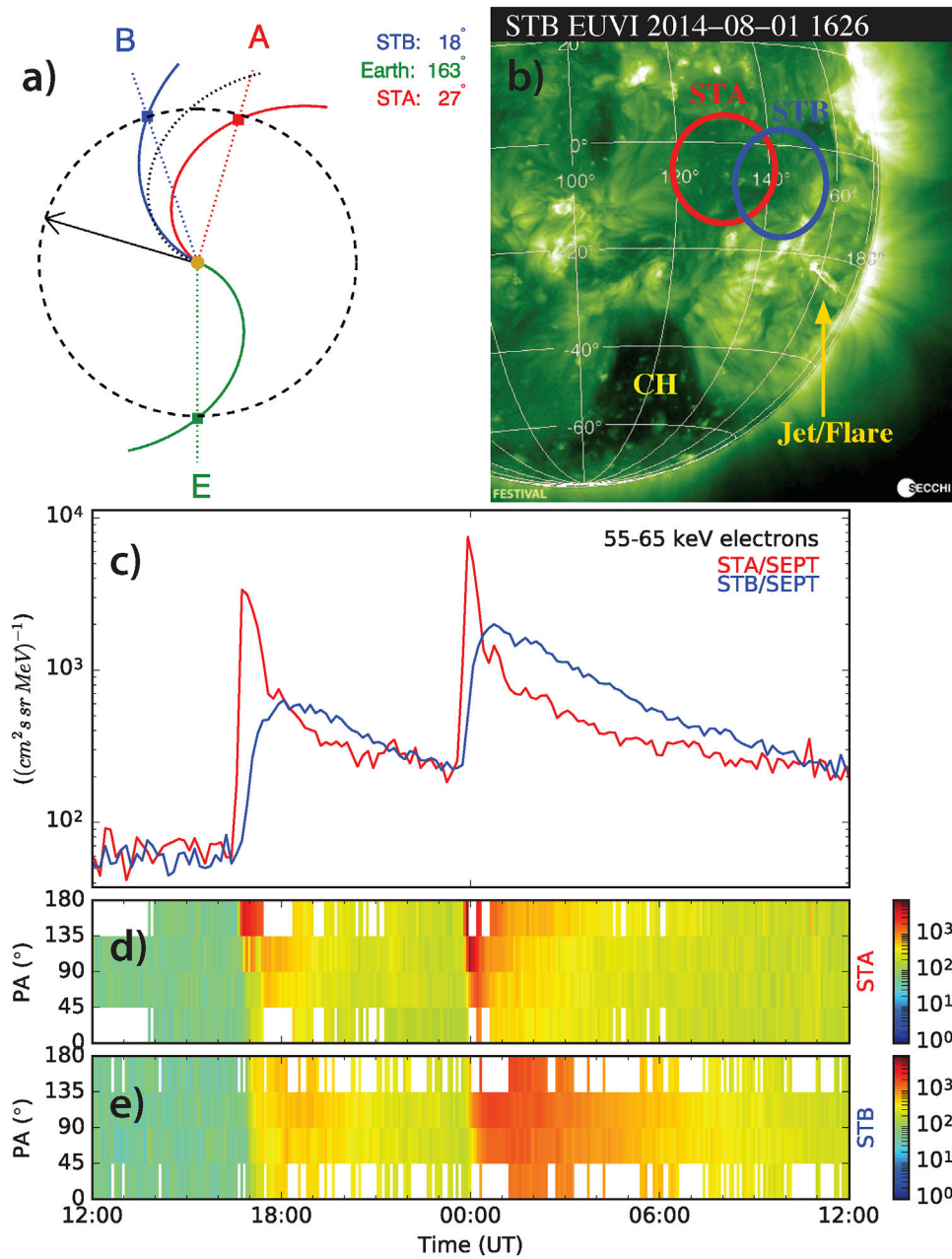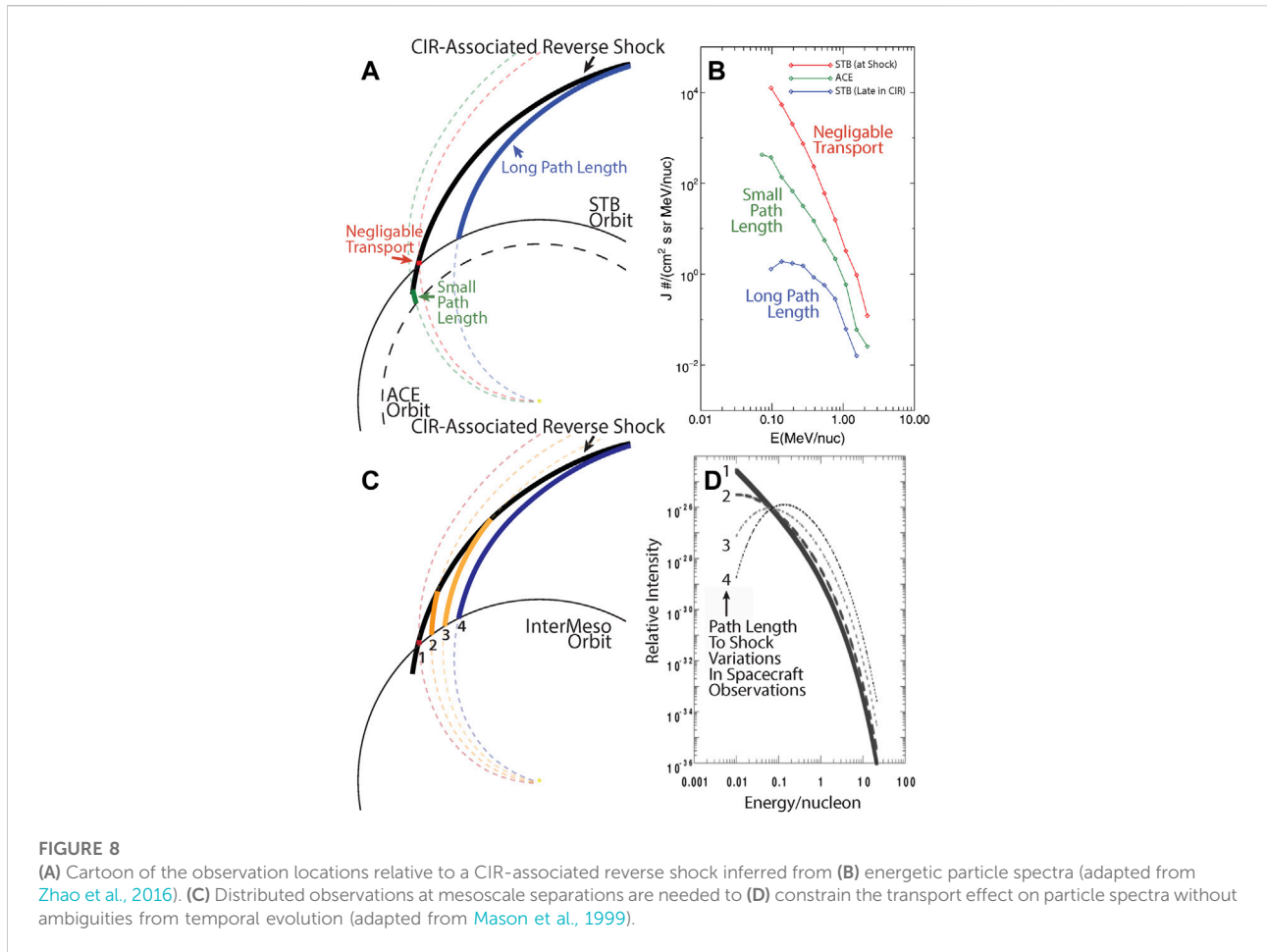
FIGURE 7
(A) The location of the STEREO spacecraft during a flare event and **(B)** the approximate footpoint of both spacecraft relative to the flare site.
(C−E) Energetic electron observations at both spacecraft showing clear differences at 1 au over 10s degrees of longitude. Adapted from Klassen et al.
(2016). Transport of energetic electrons from flare sites to 1 au is complex, and requiring multi-point measurements at mesoscale separations to
constrain.

of this mesoscale variability between the solar source and Earth at 1 au. Understanding of the transition from the inertial to dissipation range of plasma turbulence from HelioSwarm, coupled with understanding of the injection to inertial range from InterMeso, would for the first time provide a broad picture of plasma variability in the mesoscale solar wind. Additionally, the European Space Agency (ESA) Vigil mission to L5 (https://www.esa.int/Space_Safety/Vigil), in partnership with the National Oceanic and Atmospheric Administration (NOAA), is planned to launch in 2027 and will include a heliospheric imager that can provide broader context for the *in situ* observations of the InterMeso mission. The potential synergies between InterMeso and upcoming missions (e.g., HelioSwarm, PUNCH, and Vigil) motivate such an architecture within the next decade.

FIGURE 8
(A) Cartoon of the observation locations relative to a CIR-associated reverse shock inferred from **(B)** energetic particle spectra (adapted from Zhao et al., 2016). **(C)** Distributed observations at mesoscale separations are needed to **(D)** constrain the transport effect on particle spectra without ambiguities from temporal evolution (adapted from Mason et al., 1999).
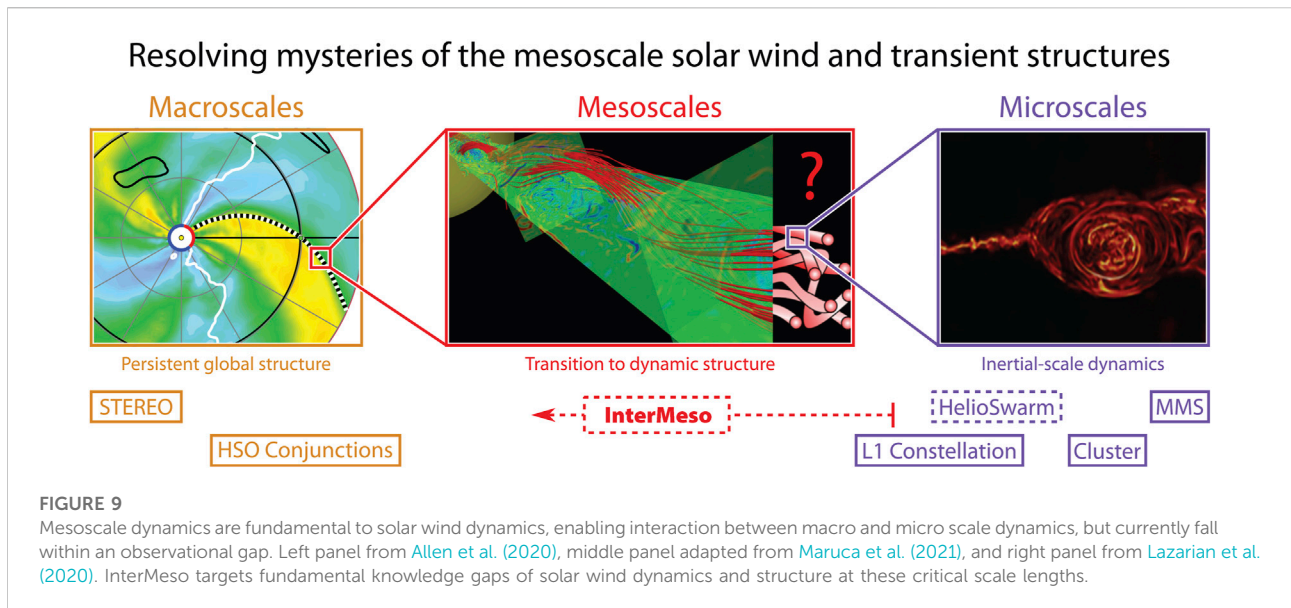
The InterMeso concept

InterMeso science traceability

The overarching science goals of InterMeso flow into eight targeted science questions, shown in the Science Traceability Matrix (STM) provided in Table 1. Addressing these questions requires simultaneous, multi-point observations with inter-spacecraft separations ranging from ~0.5 Mkm to 10 s Mkm (i.e., 100 s R_E to a few degrees in heliographic longitude at 1 au, see Figure 2). Maintaining the constellation at a near-1 au heliocentric distance enables observations of both well-formed and still-steepening shocks of CMEs and SIR/CIRs.

All InterMeso spacecraft require measurements of the low-energy, bulk solar wind plasma. This includes sub-minute cadence observations of the bulk proton population for speeds ranging from 250–1,000 km/s and densities from 1–100 cm^{-3}. This range of measurements with necessary accuracy can be accomplished with modern Faraday Cup instrumentation (e.g., Case et al., 2020). Thermal ion (1–10's keV/e) composition measurements on a less than few minute cadence will be

critical to disambiguate changes in flux tube composition. This will require the ability to distinguish between various species and charge states including H, He^{2+}, C^{5-6+}, N^{5-6+}, O^{6-7+}, and Fe^{6-12+} and can be satisfied by modern iterations of the Ulysses and ACE Solar Wind Ion Composition Spectrometer (SWICS) instrument design (Gloeckler et al., 1992). Low-energy electron observations spanning from a few eV to tens keV, i.e., including the core, halo, and strahl populations, are also needed and be achieved with the inclusion of a Parker Solar Probe (PSP) Solar Probe Analyzers-Electrons (SPAN-E)-type instrument (Kasper et al., 2016).

Additionally, suprathermal and energetic ion/electron measurements are required to explore anisotropies and, importantly, differentiate various ion species for investigating mass-per-charge-dependent processes of particle acceleration and transport. Suprathermal ion (5–100 keV/nuc) and energetic ion (0.1–10 MeV/nuc) measurements with mass determination (i.e., H, ^{3}He, ^{4}He, C, N, O, Fe) are required on a cadence of several minutes and tens of minutes, respectively, which is within the capabilities of current generation versions of the Solar Orbiter Suprathermal Ion Spectrograph (SIS;

FIGURE 9
Mesoscale dynamics are fundamental to solar wind dynamics, enabling interaction between macro and micro scale dynamics, but currently fall within an observational gap. Left panel from Allen et al. (2020), middle panel adapted from Maruca et al. (2021), and right panel from Lazarian et al. (2020). InterMeso targets fundamental knowledge gaps of solar wind dynamics and structure at these critical scale lengths.

Rodríguez-Pacheco et al., 2020; Wimmer-Schweingruber et al., 2021) instrument. Energetic electron observations (few tens keV to few MeV) are needed with capabilities of determining first-order anisotropy on a few second cadence to characterize mesoscale variations in SEP events, which can be achieved with Solar Orbiter Energetic Particle Telescope (EPT)-like instrumentation (Rodríguez-Pacheco et al., 2020; Wimmer-Schweingruber et al., 2021).

To probe mesoscale magnetic structuring and impacts of plasma waves and turbulence on particle transport, observations of the magnetic field and radio emissions released from flare events and shock acceleration are required. Vector magnetic field measurements must have a full-scale range of at least +/− 100 nT with 0.1 nT or better resolution at cadences of 16–64 vectors/sec, obtainable by current fluxgate instrumentation (e.g., PSP/FIELDS; Bale et al., 2016). Radio wave observations ranging from 10^{-18}—10^{-12} V^2/m^2/Hz over the frequency range of 0.1 kHz–20 MHz, achievable with STEREO-SWAVES (Bougeret et al., 2008) or Solar Orbiter Radio Plasma Waves (RPW; Maksimovic et al., 2020)-type instrumentation, are also needed. Accurate timing and characterization of electron acceleration near the solar surface necessitates observations of hard X-rays with an indirect imager (e.g., Krucker et al., 2020) along with radio wave observations to determine both the source location and electron characteristics. The X-ray instrument must measure hard X-ray spectra, images, and time series with an energy range between 5–100 keV, and is achievable with Solar Orbiter Spectrometer Telescope for Imaging X-rays (STIX)-type instrumentation (Krucker et al., 2020).

As such, the baseline payload for this mission requires each spacecraft of the constellation to be outfitted with: 1) bulk solar wind instrument, 2) thermal ion composition instrument, 3) suprathermal ion composition telescope, 4) energetic ion composition telescope, 5) low energy electron instrumentation, 6) energetic electron telescopes, 7) DC vector magnetic field sensor, and 8) high-frequency electric field radio wave instrumentation. Additionally, only one of the spacecraft must be equipped with 9) a hard X-ray indirect imager due to the relatively close separation needed for the InterMeso spacecraft to span the mesoscale regime.

Closure of the science objectives given in Table 1 requires simultaneous multipoint observations with longitudinal separations that span the range of mesoscale dynamics in the solar wind at 1 au. Figure 10 illustrates the ability to reconstruct longitudinal variations following either a Gaussian (top) or sigmoidal (bottom) distribution by taking a representative distribution (dashed line) and placing 1,000 randomly-placed constellations of equally-spaced observing points within the domain. For the Gaussian reconstructions, a single spacecraft can only result in a single value, two spacecraft can provide a linear variation, three spacecraft provide a quadratic, while four and more spacecraft can constrain different orders of Gaussian fits. Similarly, the sigmoidal distribution can be represented by a single value, linear fit, quadratic fit, or sigmoidal fit. As demonstrated in Figure 10, increasing the number of spacecraft increases the ability to discern characteristic longitudinal profiles relevant to structures in the solar wind, particularly Gaussian-type distributions (i.e., the spread of energetic particles from an acceleration region) and sigmoidal-type variations (i.e., current sheets or changes in topology across flux tubes). Distinguishing more complex topological variabilities, such as "ripples" in a large-scale shock structure (e.g., Bale et al., 1999), or better constraining the non-planarity and radius of curvature of interplanetary shocks (e.g.,
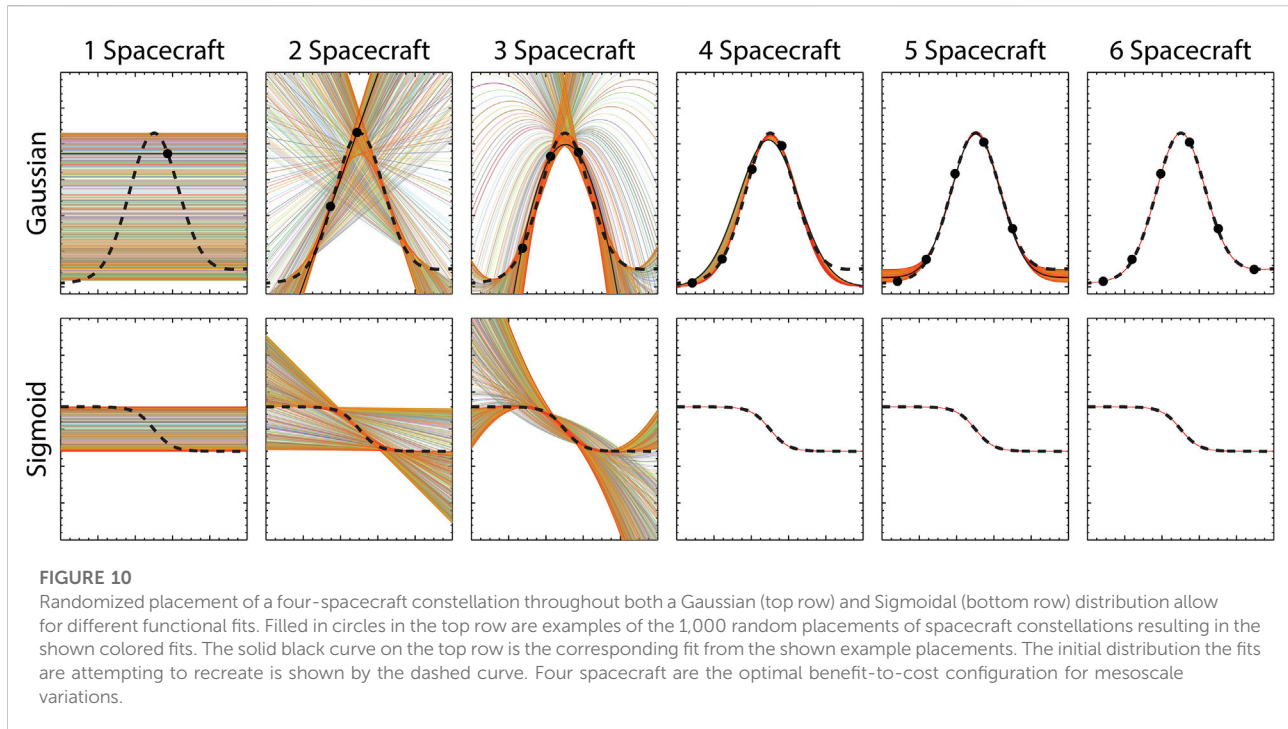
TABLE 1 InterMeso STM. Instruments: 1) bulk solar wind, 2) thermal ion composition, 3) suprathermal ion composition, 4) energetic ion composition, 5) low-energy electrons, 6) energetic electrons, 7) magnetic field, 8) radio waves, and 9) hard X-rays.

Obj	Targeted science questions	Science requirement	Measurement requirements		
			Instruments required	Inter-S/C separations	Supporting observations & models
1. Characterize and identify the origin of the mesoscale variability of the background solar wind and transient solar wind structures	1.1 What do the predominant scale sizes of the mesoscale solar wind and IMF reveal about the origins of these structures?	Conduct correlation analysis between spacecraft to determine the relevant scale sizes of the solar wind and fluxtubes. Need the ability to discern when changing between flux tubes: proton entropy, ion composition (tied to source), strahl electron properties. Compare these scale sizes to expected solar variability (i.e., from granule/supergranule) vs. variability caused by dynamics in the inner heliosphere.	1, 2, 5, 7, 8	~5.5e5 km (flux tube cross-section) ~2e6–6.5e6 km (granule/super-granule expansion at 1 au)	Solar Magnetogram DKIST (and other remote solar observatories) Simulation advancements to resolve mesoscales Connectivity tools
	1.2 How do large-scale, persistent structures transition into dynamic turbulence?	Measure the azimuthal turbulence both within and across flux tubes encompassing the inertial and injection range. Distinguish periods dominated by Alfvénic and slow-mode-like fluctuations. Determine potential differences in azimuthal turbulence in longitudinally-separated parcels of plasma with composition measurements to identify different solar sources.	1, 2, 5, 7, 8	~4e5 km during calibration 1e6–1e9 km	PUNCH as input Inputs from L1 and L5 Global MHD and flux rope simulations
	1.3 How do mesoscale variabilities of the solar source manifest variations in seed particle properties and composition at 1au?	Determine the thermal/suprathermal ion spectra for main species (H, He, C, O, Fe) at high time cadence under both quiescent solar wind and across boundaries. Use locally accelerated particles in ESP events or at CIRs to understand the role of seed particles in suprathermal-to-energetic ion composition. Constrain mesoscale variations in these populations compared to solar wind structures (1.1). Determine if the mesoscale structuring of background solar wind maps to variability in seed particle populations. Determine if this points to variability of seed particle production in different solar structures (i.e., granules), or if this is from a broader reservoir.	1, 2, 3, 4, 5, 7	~5.5e5 km (flux tube cross-section) ~2e6–6.5e6 km (granule/super-granule expansion at 1 au)	Solar imaging Solar magnetogram CIR modeling (data assimilation into MHD)
	1.4 How does the mesoscale solar wind imprint itself on solar wind transients and interplanetary shock structures?	Determine morphological variability of transient structures (such as IP shocks, CMEs) expanding into the mesoscale solar wind. Determine if the variability across transient structures and shocks match that of the background solar wind (1.1) or if there are higher order perturbations or constraints. Need ability to discern connection to source (shock or the Sun) through strahl/energetic electrons.	1, 2, 5, 6, 7, 8, 9	~5.5e5 km (flux tube cross-section) ~2e6–6.5e6 km (granule/super-granule expansion at 1 au)	L5-based and STEREO heliographic imager Ground-based radio arrays Simulation advancements to resolve mesoscales

TABLE 1 (*Continued*) InterMeso STM. Instruments: 1) bulk solar wind, 2) thermal ion composition, 3) suprathermal ion composition, 4) energetic ion composition, 5) low-energy electrons, 6) energetic electrons, 7) magnetic field, 8) radio waves, and 9) hard X-rays.

Obj	Targeted science questions	Science requirement	Measurement requirements		
			Instruments required	Inter-S/C separations	Supporting observations & models
2. Characterize and understand the impact of these mesoscale variations on particle acceleration and transport	2.1 How does mesoscale solar wind variability and intermittency impact variability in particle acceleration?	Compare mesoscale variations in the suprathermal and energetic particle range to possible variations in wave instability occurrence predictions such as lower-hybrid waves, magnetosonic waves, ion-acoustic waves, electron cyclotron drift instability, and Langmuir waves. Compare mesoscale variations in suprathermal and energetic particles to evidence of solar wind intermittency.	1, 2, 3, 4, 5, 6, 7, 8	~5.5e5 km (flux tube cross-section) ~2e6–6.5e6 km (granule/super-granule expansion at 1 au)	Simulation advancements to resolve mesoscales
	2.2 How does mesoscale structuring of solar wind transients and interplanetary shocks affect particle acceleration?	Determine mesoscale variations in longitudinally spread signatures of shock drift acceleration, diffusive shock acceleration, and fast Fermi processes to constrain the extent that mesoscale structuring may modulate these processes. Need ability to discern plasma variations across shocks, and measure variations in A/Q for energetic ions.	1, 2, 3, 4, 5, 6, 7, 8	~3e5–1e7 km (nominal IP shock radius of curvature) 1's deg (CIR interfaces, connection to reverse shocks)	L5-based and STEREO heliographic imager Ground-based radio arrays Simulation advancements to resolve mesoscales
	2.3 How do mesoscale variations of the background solar wind impact the connectivity of an observer to the solar source or acceleration site?	Ability to examine the timing of hard X-rays and the timing of *in situ* electrons to determine transit time from most probable flare location and time. Determine mesoscale variations in the injection timing and path length of energetic particles from source to observer and compare this to changes in particle population properties. Determine mesoscale variability in ion drop out events.	1, 2, 3, 4, 5, 6, 7, 8, 9	1's deg (CIR interfaces, connection to reverse shocks)	Solar Magnetogram Solar remote sensing observations Connectivity Tools Transport models
	2.4 How do mesoscale dynamics such as field line meandering and stochastic motion affect diffusion of particles in the solar wind?	Ability to detect energetic electrons with refined time resolution at multiple spacecraft separated in longitude. Determine mesoscale variability in ion drop out events.	1, 2, 3, 4, 5, 6, 7, 8, 9	1's deg (full span ~10 deg)	Stochastic motion models with particle transport

FIGURE 10
Randomized placement of a four-spacecraft constellation throughout both a Gaussian (top row) and Sigmoidal (bottom row) distribution allow for different functional fits. Filled in circles in the top row are examples of the 1,000 random placements of spacecraft constellations resulting in the shown colored fits. The solid black curve on the top row is the corresponding fit from the shown example placements. The initial distribution the fits are attempting to recreate is shown by the dashed curve. Four spacecraft are the optimal benefit-to-cost configuration for mesoscale variations.

Neugebauer and Giacalone, 2005), also benefit from increasing numbers of longitudinally-separated observations.

While additional spacecraft can increase the science return of InterMeso, four points of measurement within relevant scales provide the highest benefit-to-cost for expected variability of mesoscale phenomena with features manifesting as either a Gaussian or sigmoidal distribution (shown in Figure 10). With fewer than four spacecraft, the ability to reconstruct the distribution becomes significantly deteriorated. However, while a constellation with more than four spacecraft can serve to hone the resulting reconstructions of longitudinal variation in mesoscale phenomena, the added value, particularly when including available mission resources and cost, diminishes with additional spacecraft. As such, the InterMeso mission architecture targets four spacecraft as a baseline to determine spatiotemporal variations and elucidate mesoscale structure.

InterMeso spacecraft, orbit, and separation scales

Key to the science of InterMeso, the mission requires multiple, longitudinally-separated spacecraft in the solar wind near 1 au with varying inter-spacecraft separations over the course of the mission. In family with spacecraft missions in development and in prime operations, the prime mission phase of InterMeso is designed to last three years in order to sufficiently sample the mesoscale range in Table 1, but with systems that can remain operational likely for

several years of extended mission operation. The flexible mission design of InterMeso currently targets a 2033 launch to coincide with the ascending phase of the solar cycle but is adjustable *via* daily launch opportunities throughout the decade.

A design of the InterMeso constellation is shown in Figure 11. To reduce cost and complexity in launch, the four InterMeso spacecraft can fit on a single Evolved Expendable Launch Vehicle (EELV) Secondary Payload Adapter (ESPA)-Grande equivalent and within a standard 5 m fairing (shown in both the stowed and deployed configuration in Figure 11). All four spacecraft are launched together into heliocentric, Earth-trailing orbit, and all with the same initial drift rate before maneuvers separate the spacecraft. Figure 12A shows the initial drift rate set by the launch vehicle (green line) as well as the drift rates of each InterMeso spacecraft throughout the mission. This trajectory also maintains an inter-spacecraft separation of <0.01 au at all times while keeping the entire constellation between a heliographic distance of ~0.97 and 1.05 au over the course of the prime mission.

These drift rates allow the spacecraft to slowly separate and allow sampling of the solar wind at inter-spacecraft separations spanning the full range of mesoscale dynamics (as illustrated in Figure 2). Figure 12B illustrates the cumulative combined days at various inter-spacecraft separations for both the three-year prime mission (black line) and for the inclusion of a two-year extended mission (red-dotted line). The inclusion of the 2-years extended mission phase, especially, provides additional opportunity for sampling mesoscale structuring near the transition from the
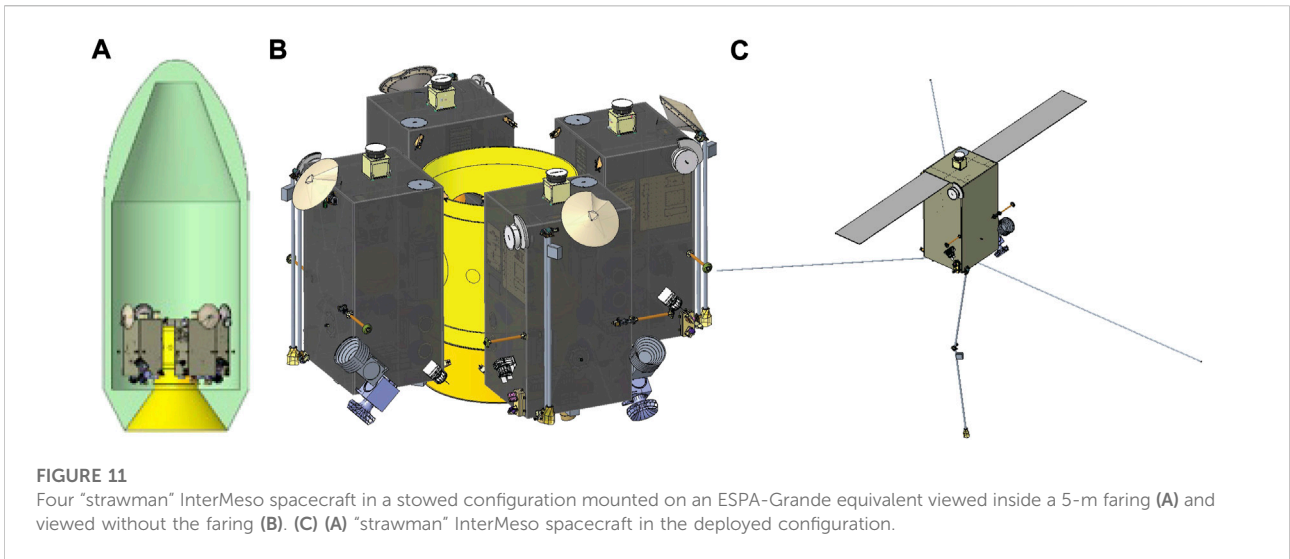
FIGURE 11
Four "strawman" InterMeso spacecraft in a stowed configuration mounted on an ESPA-Grande equivalent viewed inside a 5-m faring **(A)** and viewed without the faring **(B)**. **(C) (A)** "strawman" InterMeso spacecraft in the deployed configuration.
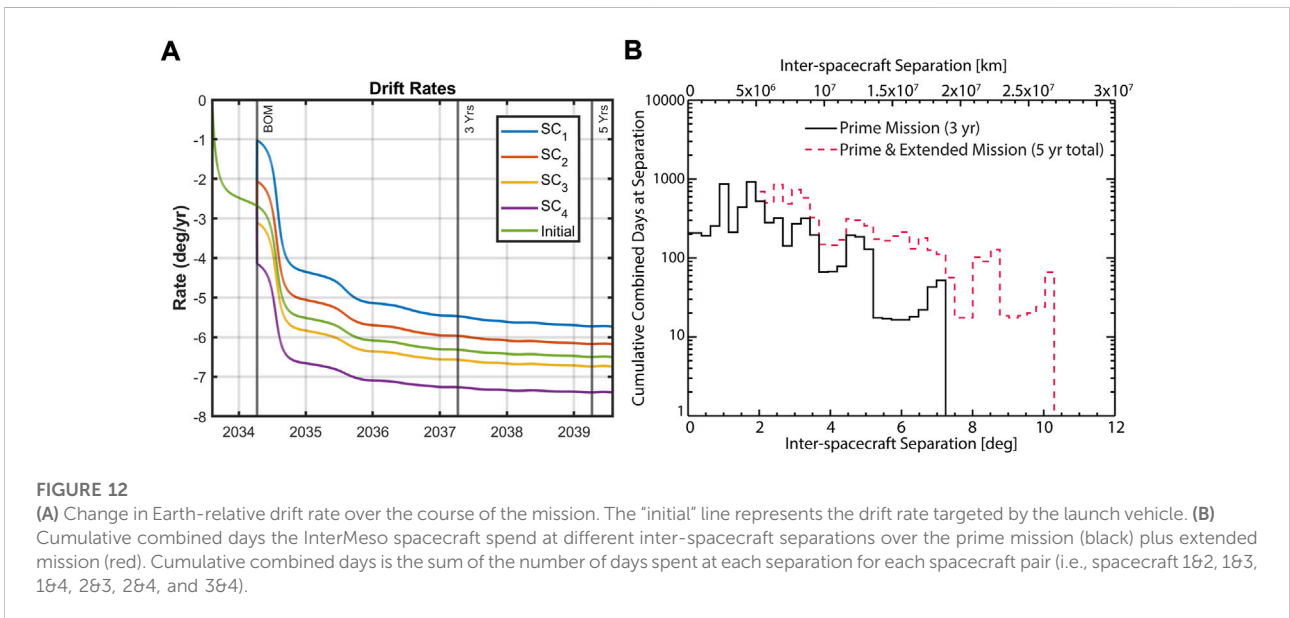

FIGURE 12
(A) Change in Earth-relative drift rate over the course of the mission. The "initial" line represents the drift rate targeted by the launch vehicle. **(B)** Cumulative combined days the InterMeso spacecraft spend at different inter-spacecraft separations over the prime mission (black) plus extended mission (red). Cumulative combined days is the sum of the number of days spent at each separation for each spacecraft pair (i.e., spacecraft 1&2, 1&3, 1&4, 2&3, 2&4, and 3&4).

inertial to the injection range; however, this additional sampling is not required for addressing the primary science goals.

Summary

The mesoscale solar wind (100s R_E to a few degrees heliographic longitude at 1 au) remains elusive in our observations, modeling frameworks, and understanding. In order to finally close this fundamental gap in our knowledge of the solar wind, new multi-point missions are required with mesoscale separations. The InterMeso mission concept provides one such solution for addressing the unresolved physics of mesoscale structure of the solar wind and transients.

Consisting of four near-identical spacecraft operating independent of one another and outfitted with a suite of particle and field instrumentation, InterMeso is designed to robustly explore the mesoscale structuring of the solar wind and its consequences on particle acceleration and transport. Operation over the three-year prime mission lifetime allow for sampling over the full range of mesoscale variability in the solar wind. The science objectives addressed by the architecture of InterMeso is achievable in the next decade, enabling advances on long-outstanding questions in heliophysics.

Data availability statement

The original contributions presented in the study are included in the article/supplementary materials, further inquiries can be directed to the corresponding author.

Author contributions

All authors listed have made a substantial, direct, and intellectual contribution to the work and approved it for publication.

Conflict of interest

The authors declare that the research was conducted in the absence of any commercial or financial relationships that could be construed as a potential conflict of interest.

Publisher's note

All claims expressed in this article are solely those of the authors and do not necessarily represent those of their affiliated organizations, or those of the publisher, the editors and the reviewers. Any product that may be evaluated in this article, or claim that may be made by its manufacturer, is not guaranteed or endorsed by the publisher.

References

Ala-Lahti, M., Ruohotie, J., Good, S., Kilpua, E. K. J., and Lugaz, N. (2020). Spatial coherence of interplanetary coronal mass ejection sheaths at 1 AU. *JGR. Space Phys.* 125, e2020JA028002. doi:10.1029/2020JA028002

Allen, R. C., Ho, G. C., Mason, G. M., Li, G., Jian, L. K., Vines, S. K., et al. (2021a). Radial evolution of a CIR: Observations from a nearly radially aligned event between Parker Solar Probe and STEREO-A. *Geophys. Res. Lett.* 48, e2020GL091376. doi:10.1029/2020GL091376

Allen, R. C., Lario, D., Odstrcil, D., Ho, G. C., Jian, L. K., Cohen, C. M. S., et al. (2020). Solar Wind Streams and Stream Interaction Regions Observed by the Parker Solar Probe with Corresponding Observations at 1 au. *Astrophys. J. Suppl. Ser.* 246, 36. doi:10.3847/1538-4365/ab578f

Allen, R. C., Mason, G. M., Ho, G. C., Rodríguez-Pacheco, J., Wimmer-Schweingruber, R. F., Andrews, G. B., et al. (2021b). Suprathermal particles from corotating interaction regions during the first perihelion pass of Solar Orbiter. *Astron. Astrophys.* 656, L2. doi:10.1051/0004-6361/202039870

Ashraf, M., and Li, G. (2019). Propagation of scatter-free solar energetic electrons in a meandering interplanetary magnetic field. *Astrophys. J.* 887, 102. doi:10.3847/1538-4357/ab4f68

Bale, S. D., Goetz, K., Harvey, P. R., Turin, P., Bonnell, J. W., Dudok de Wit, T., et al. (2016). The FIELDS instrument suite for solar probe plus. *Space Sci. Rev.* 204, 49–82. doi:10.1007/s11214-016-0244-5

Bale, S. D., Reiner, M. J., Bougeret, J.-L., Kaiser, M. L., Krucker, S., Larson, D. E., et al. (1999). The source region of an interplanetary type II radio burst. *Geophys. Res. Lett.* 26, 1573–1576. doi:10.1029/1999GL900293

Bandyopadhyay, R., Chasapis, A., Chhiber, R., Parashar, T. N., Maruca, B. A., Matthaeus, W. H., et al. (2018). Solar wind turbulence studies using MMS fast plasma investigation data. *Astrophys. J.* 866, 81. doi:10.3847/1538-4357/aade93

Bian, N. H., and Li, G. (2021). Stochastic Parker spirals in the solar wind. *Astrophys. J.* 908, 45. doi:10.3847/1538-4357/abd39a

Borovsky, J. E. (2008). Flux tube texture of the solar wind: Stands of the magnetic carpet at 1 AU? *J. Geophys. Res.* 113, A08110. doi:10.1029/2007JA012684

Bougeret, J. L., Goetz, K., Kaiser, M. L., Bale, S. D., Kellogg, P. J., Maksimovic, M., et al. (2008). S/WAVES: The radio and plasma wave investigation on the STEREO mission. *Space Sci. Rev.* 136, 487–528. doi:10.1007/s11214-007-9298-8

Burch, J. L., Moore, T. E., Torbert, R. B., and Giles, B. L. (2016). Magnetospheric Multiscale overview and science objectives. *Space Sci. Rev.* 199, 5–21. doi:10.1007/s11214-015-0164-9

Burlaga, L., Sittler, E., Mariani, F., and Schwenn, R. (1981). Magnetic loop behind an interplanetary shock: Voyager, Helios, and IMP 8 observations. *J. Geophys. Res.* 86 (8), 6673–6684. doi:10.1029/JA086iA08p06673

Case, A. C., Kasper, J. C., Stevens, M. L., Korreck, K. E., Paulson, K., Daigneau, P., et al. (2020). The solar probe Cup on the parker solar probe. *Astrophys. J. Suppl. Ser.* 246, 43. doi:10.3847/1538-4365/ab5a7b

Chen, J. H., Schwadron, N. A., Möbius, E., and Gorby, M. (2015). Modeling interstellar pickup ion distributions in corotating interaction regions inside 1 AU. *J. Geophys. Res. Space Phys.* 120, 9269–9280. doi:10.1002/2014JA020939

D'Amicis, R., Matteini, L., and Bruno, R. (2019). On the slow solar wind with high alfvénicity: From composition and micropysics to spectral properties. *Mon. Notices R. Astronomical Soc.* 483, 4. doi:10.1093/mnras/sty3329

Desai, M. I., Mitchell, D. G., Szalay, J. R., Roelof, E. C., Giacalone, J., Hill, M. E., et al. (2020). Properties of suprathermal-through-energetic He ions associated with stream interaction regions observed over the Parker Solar Probe's first two orbits. *Astrophys. J. Suppl. Ser.* 246 (2), 56. doi:10.3847/1538-4365/ab65ef

Ebert, R. W., Dayeh, M. A., Desai, M. I., and Mason, G. M. (2012). Corotating interaction region associated suprathermal helium enhancements at 1 au: Evidence for local acceleration at the compression region trailing edge. *Astrophys. J.* 749, 73. doi:10.1088/0004-637X/749/1/73

Escoubet, C. P., Fehringer, M., and Goldstein, M. (2001). <i>Introduction</i>The Cluster mission. *Ann. Geophys.* 19, 1197–1200. doi:10.5194/angeo-19-1197-2001

Farrugia, C. J., Berdichevsky, D. B., Möstl, C., Galvin, A. B., Leitner, M., Popecki, M., et al. (2011). Multiple, distant (40°) *in situ* observations of a magnetic cloud and a corotating interaction region complex. *J. Atmos. Sol. Terr. Phys.* 73, 1254–1269. doi:10.1016/j.jastp.2010.09.011

Fisk, L. A., and Gloeckler, G. (2006). The common spectrum for accelerated ions in the quiet-time solar wind. *Astrophys. J.* 640, L79–L82. doi:10.1086/503293

Fisk, L. A., and Lee, M. A. (1980). Shock acceleration of energetic particles in corotating interaction regions in the solar wind. *Astrophys. J.* 237, 620–626. doi:10. 1086/157907

Geyer, P., Temmer, M., Guo, J., and Heinemann, S. G. (2021). Properties of stream interaction regions at Earth and Mars during the declining phase of SC 24. *Astron. Astrophys.* 649, A80. doi:10.1051/0004-6361/202040162

Giacalone, J., Jokipii, J. R., and Kóta, J. (2002). Particle acceleration in solar wind compression regions. *Astrophys. J.* 573 (2), 845–850. doi:10.1086/340660

Gloeckler, G., Geiss, J., Balsinger, H., Bedini, P., Cain, J. C., Fischer, J., et al. (1992). The solar wind ion composition spectrometer. *Astron. Astrphys. Suppl.* 92, 267–289.

Hu, J., Li, G., Fu, S., Zank, G., and Ao, X. (2018). Modeling a single SEP event from multiple vantage points using the iPATH model. *Astrophys. J.* 854, L19. doi:10.3847/ 2041-8213/aaabc1

Jian, L. K., Luhmann, J. G., Russell, C. T., and Galvin, A. B. (2019). Solar terrestrial Relations observatory (STEREO) observations of stream interaction regions in 2007→2016: Relationship with heliospheric current sheets, solar cycle variations, and dual observations. *Sol. Phys.* 294, 31. doi:10.1007/s11207-019-1416-8

Jian, L. K., Russell, C. T., Luhmann, J. G., Skoug, R. M., and Steinberg, J. T. (2008). Evolution of solar wind structures from 0.72 to 1 AU. *Adv. Space Res.* 41, 259–266. doi:10.1016/j.asr.2007.03.023

Joyce, C. J., McComas, D. J., Schwadron, N. A., Christian, E. R., Wiedenbeck, M. E., McNutt, R. L., et al. (2021). Time evolution of stream interaction region energetic particle spectra in the inner heliosphere. *Astron. Astrophys.* 650, L5. doi:10.1051/ 0004-6361/202039330

Kaiser, M. K., Kucera, T. A., Davila, J. M., Cyr, O. C. S., Guhathakurta, M., and Christian, E. (2008). The STEREO mission: An introduction. *Space Sci. Rev.* 136, 5–16. doi:10.1007/s11214-007-9277-0

Kasper, J. C., Abiad, R., Austin, G., Balat-Pichelin, M., Bale, S. D., Belcher, J. W., et al. (2016). Solar wind electrons alphas and protons (SWEAP) investigation: Design of the solar wind and coronal plasma instrument suite for solar probe plus. *Space Sci. Rev.* 204, 131–186. doi:10.1007/s11214-015-0206-3

Kilpua, E. K., Pomoell, J., Vourlidas, A., Vainio, R., Luhmann, J., Li, Y., et al. (2009). STEREO observations of interplanetary coronal mass ejections and prominence deflection during solar minimum period. *Ann. Geophys.* 27, 4491–4503. doi:10.5194/angeo-27-4491-2009

Klassen, A., Dresing, N., Gómez-Herrero, R., Heber, B., and Müller-Mellin, R. (2016). Unexpected spatial intensity distributions and onset timing of solar electron events observed by closely spaced STEREO spacecraft. *Astron. Astrophys.* 593, A31. doi:10.1051/0004-6361/201628734

Knock, S. A., Cairns, I. H., Robinson, P. A., and Kuncic, Z. (2003). Theoretically predicted properties of type II radio emission from an interplanetary foreshock. *J. Geophys. Res.* 108, 1126. doi:10.1029/2002JA009508

Kollhoff, A., Kouloumvakos, A., Lario, D., Dresing, N., Gómez-Herrero, R., Rodriguez-Garcia, L., et al. (2021). The first widespread solar energetic particle event observed by Solar Orbiter on 2020 November 29. *Astron. Astrophys.* 656, A20. doi:10.1051/0004-6361/202140937

Koval, A., and Szabo, A. (2010). Multispacecraft observations of interplanetary shock shapes on the scales of the Earth's magnetosphere. *J. Geophys. Res.* 115, A12105. doi:10.1029/2010JA015373

Krucker, S., Hurford, G. J., Grimm, O., Kögl, S., Gröbelbauer, H.-P., Etesi, L., et al. (2020). The spectrometer/telescope for imaging X-rays (STIX). *Astron. Astrophys.* 642, A15. doi:10.1051/0004-6361/201937362

Lazarian, A., Eyink, G. L., Jadari, A., Kowal, G., Li, H., Xu, S., et al. (2020). 3D turbulent reconnection: Theory, tests, and astrophysical implications. *Phys. Plasmas* 27, 012305. doi:10.1063/1.5110603

Li, G., Zhao, L., Wang, L., Liu, W., and Wu, X. (2020). Identification of two distinct electron populations in an impulsive solar energetic electron event. *Astrophys. J.* 900, L16. doi:10.3847/2041-8213/abb098

Liewer, P., Qiu, J., Vourlidas, A., Hall, J. R., and Penteado, P. (2020). Evolution of a steamer-blowout CME as observed by imagers on parker solar probe and the solar terrestrial Relations observatory. *Astron. Astrophys* 650, 1-12. doi:10.1051/0004-6361/202039641

Lugaz, N., Farrugia, C. J., Winslow, R. M., Al-Haddad, N., Galvin, A. B., Nieves-Chinchilla, T., et al. (2018). On the spatial coherence of magnetic ejecta: Measurements of coronal mass ejections by multiple spacecraft longitudinally separated by 0.01 au. *Astrophys. J.* 864, L7. doi:10.3847/2041-8213/aad9f4

Maksimovic, M., Bale, S. D., Chust, T., Khotyaintsev, Y., Krasnoselskikh, V., Kretzschmar, M., et al. (2020). The solar orbiter radio and plasma waves (RPW) instrument. *Astron. Astrophys.* 642, A12. doi:10.1051/0004-6361/201936214

Maruca, B. A., Rueda, J. A. A., Bandyopadhyay, R., Bianco, F. B., Chasapis, A., Chhiber, R., et al. (2021). MagneToRE: Mapping the 3-D magnetic structure of the solar wind using a large constellation of nanosatellites. *Front. Astron. Space Sci.* 8, 665885. doi:10.3389/fspas.2021.665885

Mason, G. M., Desai, M. I., Mall, U., Korth, A., Bucik, R., von Rosenvinge, T. T., et al. (2009). *In situ* observations of CIRs on STEREO, wind, and ACE during 2007 – 2008. *Sol. Phys.* 256, 393–408. doi:10.1007/s11207-009-9367-0

Mason, G. M., and Sanderson, T. R. (1999). CIR associated energetic particles in the inner middle heliosphere. *Space Sci. Rev.* 89, 77–90. doi:10.1023/A: 1005216516443

Mason, G. M., Von Steiger, R., Decker, R. B., Desai, M. I., Dwyer, J. R., Fisk, L. A., et al. (1999). "Origin, injection, and acceleration of CIR particles: Observations," in *Corotating interaction regions*. Editors A. Balogh, J. T. Gosling, J. R. Jokipii, R. Kallenbach, and H. Kunow (Dordrecht: Springer), 7. Space Sciences Series of ISSI. doi:10.1007/978-94-017-1179-1_16

Mazur, J. E., Mason, G. M., Dwyer, J. R., Giacalone, J., Jokipii, J. R., and Stone, E. C. (2000). Interplanetary magnetic field line mixing deduced from impulsive solar flare particles. *Astrophys. J.* 532, L79–L82. doi:10.1086/312561

Murphy, N., Smith, E. J., and Schwadron, N. A. (2002). Strongly underwound magnetic fields in co-rotating rarefaction regions: Observations and implications. *Geophys. Res. Lett.* 29 (22), 23-1–23-4. doi:10.1029/2002GL015164

Neugebauer, M., Giacalone, J., Chollet, E., and Lario, D. (2006). Variability of low-energy ion flux profiles on interplanetary shock fronts. *J. Geophys. Res.* 111, A12107. doi:10.1029/2006JA011832

Neugebauer, M., and Giacalone, J. (2005). Multispacecraft observations of interplanetary shocks: Nonplanarity and energetic particles. *J. Geophys. Res.* 110, A12106. doi:10.1029/2005JA011380

Owens, M. J., Lockwood, M., and Barnard, L. A. (2017). Coronal mass ejections are not coherent magnetohydrodynamic structures. *Sci. Rep.* 7, 4152. doi:10.1038/ s41598-017-04546-3

Perrone, D., Stansby, D., Horbury, T. S., and Matteini, L. (2019). Radial evolution of the solar wind in pure high-speed streams: HELIOS revised observations. *Mon. Not. R. Astron. Soc.* 483, 3730–3737. doi:10.1093/mnras/sty3348

Pulupa, M., and Bale, S. D. (2008). Structure on interplanetary shock fronts: Type II radio burst source regions. *Astrophys. J.* 676, 1330–1337. doi:10.1086/526405

Richter, A. K., and Luttrell, A. H. (1986). Superposed epoch analysis of corotating interaction regions at 0.3 and 1.0 AU: A comparative study. *J. Geophys. Res.* 91 (5), 5873–5878. doi:10.1029/JA091iA05p05873

Roberts, O. W., Nakamura, R., Torkar, K., Narita, Y., Holmes, J. C., Voros, Z., et al. (2020). Sub-ion scale compressive turbulence in the solar wind: MMS spacecraft potential observations. *Astrophys. J. Suppl. Ser.* 250, 35. doi:10.3847/ 1538-4365/abb45d

Rodríguez-Pacheco, J., Wimmer-Schweingruber, R. F., Mason, G. M., Ho, G. C., Sánchez-Prieto, S., Prieto, M., et al. (2020). The energetic particle detector: Energetic particle instrument suite for the solar orbiter mission. *Astron. Astrophys.* 642, A7. doi:10.1051/0004-6361/201935287

Schwadron, N. A. (2002). An explanation for strongly underwound magnetic field in co-rotating rarefaction regions and its relationship to footpoint motion on the the sun. *Geophys. Res. Lett.* 29 (14), 8-1–8-4. doi:10.1029/2002GL015028

Schwadron, N. A., Joyce, C. J., Aly, A., Cohen, C. M. S., Desai, M. I., McComas, D. J., et al. (2020). A new view of energetic particles from stream interaction regions observed by Parker Solar Probe. *Astron. Astrophys.* 650, A24. doi:10.1051/0004-6361/202039352

Schwenn, R. (1990). "Large-scale structure of the interplanetary medium," in *Physics of the inner heliosphere I. Physics and chemistry in space, space and solar physics*. Editors R. Schwenn and E. Marsch (Berlin, Heidelberg: Springer), 20. doi:10.1007/978-3-642-75361-9_3

Tritschler, A., Rimmele, T. R., Berukoff, S., Casini, R., Kuhn, J. R., Lin, H., et al. (2016). Daniel K. Inouye solar telescope: High-resolution observing of the dynamic sun. *Astron. Nachr.* 337, 1064–1069. doi:10.1002/asna.201612434

Verscharen, D., Klein, K. G., and Maruca, B. A. (2019). The multi-scale nature of the solar wind. *Living Rev. Sol. Phys.* 16, 5. doi:10.1007/s41116-019-0021-0

Wimmer-Schweingruber, R. F., Janitzek, N. P., Pacheco, D., Cernuda, I., Espinosa Lara, F., Gomez-Herrero, R., et al. (2021). First year of energetic particle measurements in the inner heliosphere with Solar Orbiter's Energetic Particle Detector. *Astron. Astrophys.* 656, A22. doi:10.1051/0004-6361/202140940

Zhao, L., Li, G., Ebert, R. W., Dayeh, M. A., Desai, M. I., Mason, G. M., et al. (2016). Modeling transport of energetic particles in corotating interaction regions: A case study. *JGR. Space Phys.* 121, 77–92. doi:10.1002/2015JA021762

Zhao, L., Li, G., Zhang, M., Wang, L., Moradi, A., and Effenberger, F. (2019). Statistical analysis of interplanetary magnetic field path lengths from solar energetic electron events observed by WIND. *Astrophys. J.* 878, 107. doi:10.3847/1538-4357/ab2041